Eur. J. Med. Chem. 33 (1998) 625–633

A CoMFA investigation of sigma receptor binding affinity: Reexamination of a spurious sigma ligand

Seth Y. Ablordeppey[a]*, Mahmoud El-Ashmawy[b], James B. Fischer[c], Richard A. Glennon[b]

[a]*College of Pharmacy & Pharmaceutical Sciences, Florida A & M University, Tallahassee, FL 32307, USA*
[b]*Department of Medicinal Chemistry, School of Pharmacy, Medical College of Virginia, Virginia Commonwealth University, Richmond, VA 23298, USA*
[c]*Cambridge NeuroScience Inc., Cambridge, MA 02139, USA*

(Received 1 September 1997; accepted 5 March 1998)

Abstract – A comparative molecular field analysis (CoMFA) investigation was conducted on the binding of 64 compounds to σ_1 receptors. Although CoMFA accurately predicted the binding affinities of the 64 compounds in the final set ($R^2 = 0.989$), it was unable to predict the high affinity of the previously reported bridged σ ligand SC-50691. SC-50691, and its *endo* and *exo* isomers were synthesized and found to bind with much lower affinity than was previously reported. © Elsevier, Paris

sigma ligands / CoMFA / QSAR / piperidinobenzonorbornane / PLS analysis

1. Introduction

Sigma (σ) receptors remain an attractive target for drug design because of their possible involvement in schizophrenia, regulation of motor behavior, convulsions, anxiety, and other CNS-related disorders [1, 2]. More recently, there appears to be an emerging role for sigma receptors in cholesterol biosynthesis [3]. We have previously reported on the synthesis, binding affinity and 3D-QSAR of σ receptor ligands in order to better understand the structural requirements for sigma receptor binding [4-9]. Since that time, however, it has become accepted that there exist at least two populations of σ receptors: σ_1 and σ_2 [2]. Certain benzomorphans, such as (+)-pentazocine, bind in a fairly selective manner at σ_1 sites [2]; at this time, there are no σ_2-selective agents. As radioligands for the σ_1 site became available, we also reported on the structural features important for σ_1 receptor binding especially as they apply to phenylalkylamines [10] (see *figure 1*).

Indeed, two independent investigations reached the same conclusions regarding binding requirements even though the two studies used different types of compounds [11, 12]. More recent interest in the development of sigma receptor ligands appears to be focussed on obtaining selective ligands for the σ receptors [13-16]. Because of the diverse structural features tolerated at the σ_1 sites [1, 2], it became apparent that a model of σ_1 receptor binding would be useful for estimating the activity of potential ligands prior to synthesis. Due to the similar

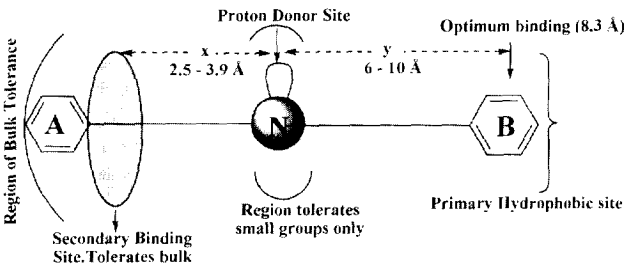

Figure 1. Receptor features presumed to be important for σ_1 binding {reprinted from Glennon et al. [10]}. The receptor likely consists of a primary hydrophobic site (B) situated 6 to 10 Å (distance *y*) from an amine binding site (N), a secondary binding site situated 2.5 to 3.9 Å (distance *x*) from the amine site, and a region of bulk tolerance associated with the secondary site.

*Correspondence and reprints

structural requirements for 'overall σ receptor' binding (using the σ_1/σ_2 non-selective [^{3}H]DTG as radioligand) and σ_1 receptor binding (using [^{3}H]-(+)-pentazocine as radioligand), and because CoMFA [9, 18] analysis seemed to explain the binding properties of these agents to σ sites [9], we undertook a CoMFA analysis for σ_1 binding. We now take this opportunity to describe this CoMFA model for σ_1 binding.

Application of the derived CoMFA model to predict the binding affinity of the most potent sigma agent reported in the literature [19] i.e., SC-50691, **65**:

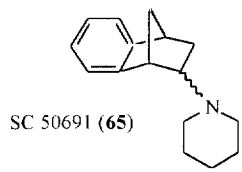

SC 50691 (**65**)

showed this compound to be a curious outlier. The hypothesis for optimum σ binding [10] was not satisfied in SC-50691. Furthermore, the present model predicts the *endo* and the *exo* isomers not to bind with high affinity at the σ_1 receptors. However, because previous reports suggest that pronounced pharmacological differences may arise from minor structural changes in conformationally defined benzonorbornane derivatives [20], it was of interest to investigate the possibility that SC-50691 may possess unique structural features that may be related to the very high affinity reported by Cheng et al. [19]. Thus, to explore the possibility that the benzonorbornane structure may introduce additional information necessary for developing a novel pharmacophore for σ receptor sites, we synthesized SC-50691 and its *endo* and *exo* isomers and examined their binding at the σ receptor sites:

2. Molecule building

Phenylalkylamines are quite conformationally flexible molecules; in order to restrict the available conformational space, two assumptions were made in the selection of appropriate conformations for the molecules modeled in this study. The first assumption is related to the pharmacophore elements in most σ ligands. Visual inspection of σ_1 receptor ligands suggests at least three pharmacophoric groups: (i) a phenyl-B ring which occupies a primary hydrophobic site, (ii) a nitrogen atom which is preferably substituted by hydrogen or a small alkyl group, and (iii) a somewhat longer N-alkyl group that is at least 2.5 Å in length and which may carry a phenyl-A ring [10] (see *figure 1*). The question that arises though is how these groups are arranged in three-dimensional space. To answer this question we have proposed a second working hypothesis based on previous SAR studies. Because binding affinity increases with increasing y-chain length, it is reasonable to assume that the phenyl-B ring will extend optimally to interact with the hydrophobic binding sites on the σ_1 receptor. Thus, the assumption is made that the alkyl chain carrying the phenyl-B ring lies in the extended conformation at the receptor site. Less restriction is placed on the position of phenyl-A since this region tends to tolerate bulk, and a variety of structural features are accommodated at this site.

All molecular modeling in this study was performed on a Silicon Graphics Iris Entry Indigo or Indy running the SYBYL software (Tripos Inc., version 6.0 or 6.3) with the QSAR/CoMFA modules. All molecules were constructed de novo using the SKETCH routine in SYBYL. The template molecule was (+)-pentazocine because of its fairly rigid structure. After construction of the molecule from fragments in the SYBYL library, (+)-pentazocine was minimized by Maximin 2 using the conjugate gradient method and energy change convergence criterion of 0.01 kcal/mol. The resulting structure of (+)-pentazocine was subjected to a full geometry optimization using the AM1 Hamiltonian (in SYBYL's implimentation of MOPAC 5.0) with the PRECISE option. Charges were calculated by the Gasteiger-Huckel method. This structure then served as the template on which the key phenylpentylamine (i.e. 1-(5-phenylpentyl)piperidine, compound **45**) was fit. The structure was built from fragments in SYBYL, the chain was set to the extended conformation and treated the same way as (+)-pentazocine. The coordinates of 1-(5-phenylpentyl) piperidine then served as the structure from which most of the other phenylalkylamines were constructed.

3. Molecule alignment

The RMS Fit routine was used to align all molecules to either the structure of (+)-pentazocine or compound **45** depending on the relationship between the selected compound and the two template molecules. The fitting points for the three pharmacophore elements indicated above were: (i) the centroid of the aromatic ring (phenyl-B) where available, or, in its absence, the third carbon atom from the N-atom located in the direction of that ring, (ii) the N-atom itself, and (iii) the third carbon atom of the alkyl chain or the C4-carbon atom of the piperidine ring in the direction of the second aromatic ring (phenyl-A). Once fitted, all compounds were put into

a database where their 3-D structures were generated for the CoMFA tables.

4. Development of the CoMFA model

A region was generated using the automatic molecular volume mode which ensured that all molecules were contained within a 3-D grid with the dimensions of 33 × 25 × 22. Although a 1.0 Å grid spacing used in the initial investigation showed a more favorable cross-validated R^2 value, subsequent investigations utilized a 2.0 Å grid spacing because of the limitation of computational space for 64 molecules in the CoMFA tables. Steric and electrostatic fields were sampled at the intersection of a 3-D lattice using a sp^3-hybridized carbon atom probe with a positive unit charge and a distance-dependent dielectric constant. Cut-off values were SYBYL default values. The linear equations were obtained by PLS with cross-validation groups equal to the number of molecules in the tables yielding the desired optimum number of components for the final statistics. The initial models were also compared with one obtained by sampling lipophilic fields (i.e by adding a column of log P to the CoMFA Tables) in addition to the steric and electrostatic fields but were found to provide little or no additional statistical improvements.

5. Chemistry

The synthesis of SC 50691 was acomplished by published methods starting from cyclopentadiene [22, 20]. These methods, in our hands, resulted in a mixture of the *exo* and *endo* isomers as shown by TLC and subsequently confirmed as such by comparing the nmr data with the published data of the isomers of 2-aminobenzonorbornene. Using these methods, the *exo*-2-aminobenzonorbornene **66** was obtained after column chromatography and recrystallization. Treatment of **66** with 1,5-dibromopentane in DMF, in the presence of K_2CO_3 afforded the *exo* isomer **67** in 25% yield [23]. In contrast, hydroboration-oxidation of benzonorbornadiene to the alcohol, followed by oxidation under Swerns condition afforded 2-benzonorbornenone, **68** [22]. Treatment of **68** with piperidine and sodium cyanoborohydride, under a reductive alkylation condition gave the *endo* isomer **69** as a main product. The NMR data of **67** and **69** are consistent with the configurations assigned, based in part, on the chemical shifts of the protons at C-2 and C-3 [22]. Thus, the C-2 *endo* H (δ, 2.95) of **67** appeared upfield of the C-2 *exo* H (δ, 3.78) of **69**; these are consistent with the assignments of Grunewald et al. [20].

6. Results and discussion

6.1. The initial model

A data table was created with the structures of 48 compounds (K_i range; 0.17 nM-3640 nM or > 21000-fold) (*table I*). These compounds are referred to as the Training Set. Calculations were performed using SYBYL's implementation of the PLS algorithm. When a cross-validated group of 48 and 10 PLS components were utilized, the cross-validated R^2 (R^2_{CV}) was found to be 0.615 (standard error = 0.779) corresponding to an optimum number of components of 8. Using 8 components and a minimum sigma value of 0.0, the final statistics were obtained (R^2_{noCV} = 0.994, standard error = 0.095, F = 839.3). To test the validity of this model, the binding affinities of 16 compounds (Test Set) were predicted before actual binding data became available. The structures were modeled in a similar manner to those of the Training Set and the predicted values along with the subsequent experimentally determined values are presented in *table II* in the form of pK_i values and *figure 2a*. In order to test whether the eight (8) PLS components obtained by the leave one-out procedure was overfitting the data we also ran a second PLS analysis using five (5) cross-validated groups and 10 components. The results are as follows: R^2_{CV} was found to be 0.585 (standard error = 0.778) corresponding to an optimum number of components of 5. Using the 5 components and a minimum sigma value of 0.0, the final statistics were obtained (R^2_{noCV} = 0.974, standard error = 0.193, F = 321.0). The sixteen test compounds were also predicted, yielding a regression R^2 value of 0.564 (*figure 2b*). Thus, it will appear that the statistics are more favorable with the leave-one-out approach.

6.2. The final model

Compounds in the Training Set and those in the Test Set were subsequently combined to obtain a total of 64 compounds with K_i ranging from 0.09 nM to 3640 nM or > 40000-fold. A PLS analysis was run in a similar manner as above. Using a cross-validated group of 64 and 10 PLS components, the optimal number of components was 7 and the R^2_{CV} was found to be 0.732. The optimum number of components was used for the final statistics which yielded a regression (R^2 value) of 0.989 (standard error = 0.135 and F = 721.69). *Figure 2* depicts a plot of predicted pK_i against the actual pK_i values from *table II*.

6.3. CoMFA contour maps

The CoMFA contour maps are presented in *figure 3*. These maps were obtained by extracting the standard

Table Ia. Compounds used in the initial CoMFA Table (Model A).

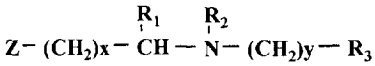

Compound	Z	x	R_1	R_2	y	R_3	K_i (nM)
1	Ph	1	CH_3[R-(−)]	H	3	Ph	10.8
2	4-I, Ph	1	CH_3[R-(−)]	H	3	Ph	18.0
3	Ph	1	H	H	4	Ph	2.6
4	Ph	0	H	H	4	Ph	9.7
5	Ph	3	H	H	5	Ph	0.48
6	Ph	0	H	H	5	Ph	0.32
7	Ph	1	H	H	3	Ph	11.0
8	Ph	1	H	H	5	Ph	0.17
9	Ph	0	H	H	7	Ph	2.3
10	Ph	1	H	H	7	Ph	1.5
11	Ph	0	H	H	5	CyH	0.8
12	Ph	2	H	H	5	Ph	0.28
13	CH_3	1	H	CH_3	5	Ph	0.29
14	Ph	1	CH_3[R-(−)]	$(CH_3)_2$	3	Ph	134
15	Ph	1	CH_3[S-(+)]	CH_3	3	Ph	1.3
16	H	0	H	CH_3	5	Ph	0.58
17	Ph	1	CH_3[S-(+)]	Bzl	3	Ph	128
18	H	0	H	H	5	CyH	6.8
19	H	0	H	CH_3	5	CyH	0.26
20	Ph	0	H	CH_3	5	Ph	0.19
21	Ph	1	CH_3[S-(+)]	H	5	Ph	0.9
22	Ph	1	CH_3[S-(+)]	H	4	Ph	19.0
23	Ph	1	CH_3[S-(+)]	H	3	Ph	51.0
24	Ph	2	H	H	3	Ph	11.0
25	Ph	1	CH_3[R-(−)]	H	3	1-Np	8.6
26	Ph	1	CH_3[R-(−)]	H	3	2-Np	5.7
27	(+)-Pentazocine						1.6
28	(−)-Pentazocine						114
29	DTG						41
30	Haloperidol						0.47
31	Ifenprodil						5.8
32	Dextromethorphan						522
33	R-Butaclamol						583
34	S-Butaclamol						69
35	(+)-NANM						148
36	(−)-NANM						3640
37	R-3PPP						48
38	S-3PPP						312
39	Perphenazine						25
40	Chlorpromazine						336
41	Rimcazole						1156

deviation coefficients from the PLS analysis and using the result to graph the contour maps. Although steric and electrostatic maps were generated only the steric maps are productive in explaining the SAR and are shown (*figure 3*). The steric maps are more useful when the compounds of interest are embedded in them. For example, *figure 3a* shows the most potent compound in the training set (compound **55**) embedded in the steric map. In these figures (*figure 3a-c*), areas where increasing bulk results in increasing activity are colored green whereas

Table Ib.

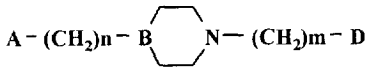

	A	*n*	B	*m*	D	K_i (nM)
42	3-Cl, Ph	0	CHOH	3	Ph	15
43	Ph	0	N	3	H	82
44	Ph	1	CH	5	Ph	0.58
45	H	0	CH	5	Ph	0.48
46	N-Methyl quaternary analog of compound **26**					2.7
47	H	0	CH	3	Ph	49
48	Ph	1	N	5	Ph	0.4

Table II. Table of test compounds with actual K_i and predicted K_i [a].

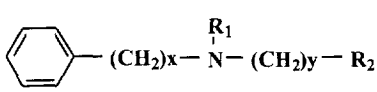

X

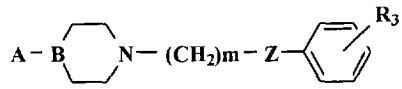

Y

Compound	Structure									Activity values (nM)	
	X				Y					Predicted pK_i	Actual pK_i
	x	R_1	*y*	R_2	A	B	*m*	Z	R_3		
49	2	H	4	CH_3						− 1.20	− 1.70
50	3	CH_3	5	Ph						+ 0.64	+ 0.42
51	2	CH_3	5	Ph						+ 0.29	+ 0.69
52	4	H	1	H						− 1.10	− 1.62
53					Ph	CH	4	CO	3-Cl	− 0.08	− 0.89
54					H	CH	4	CO	3-Cl	− 0.33	+ 0.66
55					Ph	CH	4	CO	H	− 0.11	+ 1.05
56					Ph	CH	5	–	4-Cl	+ 0.77	+ 0.82
57					Ph	CH	4	CO	4-Cl	− 0.08	+ 0.92
58					H	CH	4	CO	4-Cl	− 0.26	+ 0.74
59					Ph	CH	3	–	H	+ 0.4	+ 0.52
60					Ph	CH	4	–	H	+ 0.23	+ 0.66
61					Ph	CH	5	–	H	+ 0.72	+ 0.80
62					Ph	N	3	–	H	− 1.47	− 1.01
63										+ 0.47	+ 0.12
64										− 1.20	− 1.92

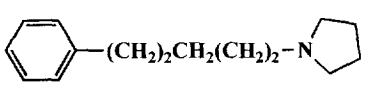

63

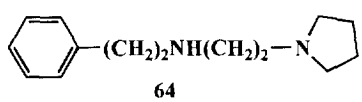

64

[a] Regression coefficient = 0.8 (R^2 = 0.65).

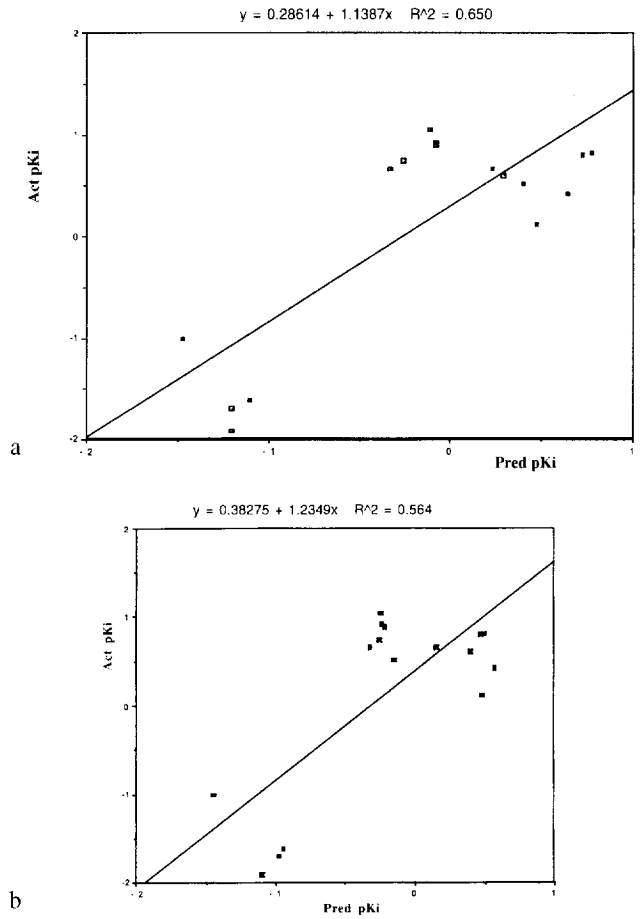

Figure 2. (a) A plot of the actual pK_i versus the predicted pK_i of test compounds in *table II* ($n = 16$), using the leave-one-out procedure and an optimum number of components of 8. (b) A plot of the actual pK_i versus the predicted pK_i of test compounds in *table II* ($n = 16$), using an optimum number of components of 5.

areas where bulk results in decrease in affinity are colored red. Compound **55** has both phenyl groups lying in the green areas (*figure 3a*) where bulk leads to increase in affinity (which corresponds to the primary and secondary hydrophobic sites at the σ receptors) and has none of its structural features in the red areas where bulk would have decreased affinity; and thus partly explains its potency. *Figure 3b* and *c* indicate that both *exo* (**67**) and *endo* (**69**) isomers of compound **65** interact only minimally with the favorable areas of the contour maps and thus supports the view that both isomers should have only low to moderate binding affinity at the σ_1 receptors. In addition, the *endo*-isomer is expected to bind with a much lower affinity than the *exo*-isomer because its phenyl ring makes no productive interaction with the green areas where substitution is expected to enhance affinity while the phenyl ring of the *exo* isomer makes a minimal interaction with the green area corresponding to the primary hydrophobic site.

6.4. *CoMFA predictions*

Examination of the test set predictions shows that phenylketones **53, 54, 55, 57** and **58** were poorly predicted while the phenylalkylamines were (except **52**) correctly predicted. One explanation for the poor prediction may be related to the hypothesis that the phenylketones as a group bind to σ_1 receptors in a manner different from that of the phenylalkylamines. A closer observation reveals that they bind with significantly higher affinities than predicted by the model; about 10 times higher affinity than their predicted binding K_i. An alternative explanation for their higher affinities is related to a favorable carbonyl interaction with the receptor which is not taken into consideration in deriving the model. This explanation is consistent with the Gulligan model [24] which specifies a hydrogen bonding center midway between the basic nitrogen and the distal hydrophobic locus. Could the carbonyl group present in the butyrophenones (compounds **53-55**, **57**, **58**) interact with this hydrogen bonding center and thus account for the 10-fold increase in affinity over predicted values? Compound **52**, although a phenylalkylamine, was expected to be poorly predicted because of its unique structure i.e., a secondary amine with a methyl group which could not interact productively with the secondary binding site of the receptor model.

The final model is intended to be used as a guide for the design of novel σ ligands. However, we became aware of the report of Cheng et al. [19] that SC-50691 binds with the highest affinity of any sigma receptor ligands: SC-50691, $K_i = 0.075$ nM. Cursory visual inspection of SC-50691 reveals that it lacks those pharmacophoric features important for high sigma binding affinity. Although the agent was originally reported as an isomeric mixture, the individual *exo* and *endo* isomers were modeled in the present study. These isomers were modeled in a manner similar to those of the other agents in the data tables and the distances from the centroid of the phenyl rings to the N-atoms were compared with our observed optimum distances. The N-centroid distance (y) for the *exo*-isomer was 5.07 Å and that of the *endo* isomer was 3.88 Å (compared with the optimum y distance of 8.3 Å [10]). Therefore, on the basis of distance values alone, SC-50691 should have only moderate to weak binding affinity, and the *exo* isomer should be expected to bind with a higher affinity than the *endo* isomer (centroid

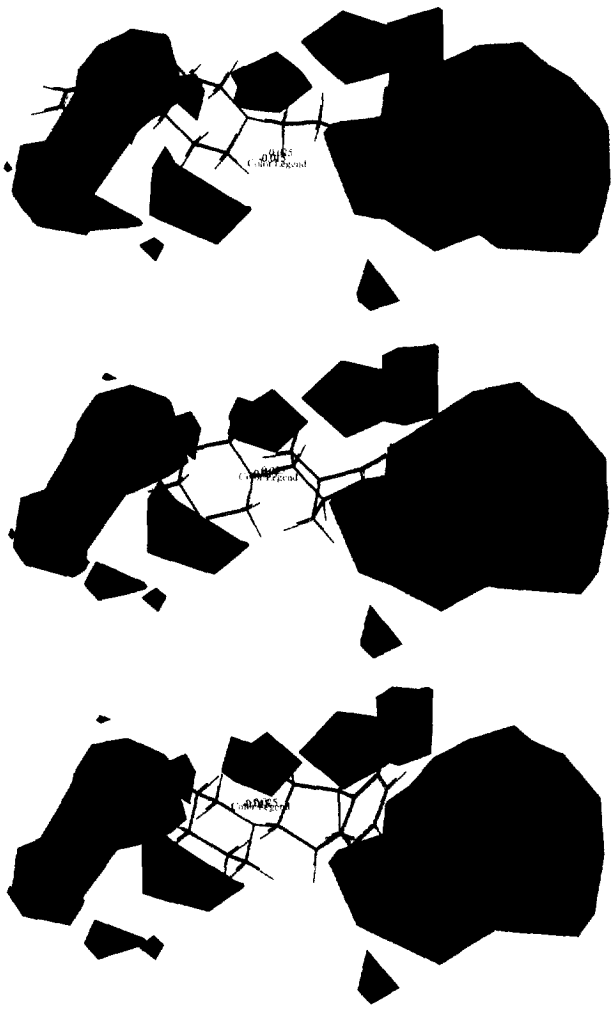

Figure 3. (a) A CoMFA steric contour map of the final model with the most potent compound (**55**) embedded. Green areas show favored areas where increasing bulk results in increasing affinity and the red contours indicate disfavored areas. Compound **55** has both phenyl groups in the favored areas corresponding to the primary and secondary hydrophobic sites. (b) The CoMFA steric contour map as in (a) but with the *exo* isomer of SC 50691 (**67**) embedded. The *exo* isomer makes only minimal contact with one of the two favored areas and was expected to bind with moderate affinity only. (c) The CoMFA steric contour map as in (a) but with the *endo* isomer of SC 50691 (**69**) embedded. The *endo* isomer makes no contact with any of the two favored areas and was expected to bind with weak or no affinity.

to N distance = 3.88 Å). CoMFA predictions were also made; *exo*-SC 50691, $K_i = 56$ nM, and *endo*-SC 50691, $K_i = 380$ nM. Based on both the distance criterion and CoMFA predictions, there is a strong suggestion that the *exo* isomer of **65** should have a higher affinity at σ_1 receptors than the *endo* isomer. These values were also significantly different from the 0.075 nM reported by Cheng et al. [19].

Table III. Comparison of σ_1 receptor ligand binding data from two different laboratories.

Compound	σ_1 K_i value [11]	σ_1 K_i value [12]	Ratio [σ_1(12)/ σ_1(11)]
Haloperidol	0.3	0.5	1.7
(+)-Pentazocine	2.0	1.7	0.85
Fluphenazine	7.6	32	4.3
DTG	12	41	3.4
R-(+)-3PPP	5	48	9.6
(−)-Butaclamol	47	69	0.68
(+)-NAMN	45	150	3.3
S-(−)-3PPP	31	310	10
Dextromethorphan	121	520	4.3

There are several possible explanations for why the CoMFA prediction of **65** is inconsistent with the reported value [19]. These range from an inability of the model to account for various structural features (i.e., no bridged compounds were included in generating the model), to a unique mode of binding for this bridged compound relative to the other compounds examined. To further explore these issues, we prepared and characterized the *exo*, *endo* and isomeric mixture of **65**.

Binding affinities of SC 50691 and its *exo* and *endo* isomers were also determined. Consistent with our predictions, **65** was found to bind with only moderate affinity ($K_i = 66 \pm 13$ nM) and the *exo*-isomer binds with a higher affinity ($K_i = 24 \pm 6$ nM; Predicted $K_i = 56$ nM) than the endo-isomer ($K_i > 1000$ nM; Predicted $K_i = 380$ nM).

We also explored the possibility that the 1000-fold difference in affinity between our binding K_i value for SC 50691 and those of Cheng et al. may be due to interlaboratory differences by evaluating the differences between data published in our laboratory [11] with those published in another laboratory [12] and which used different radioligands for their binding assays [2]. As shown in *table III*, each of the differences in K_i's is either equal or less than 10-fold; suggesting that interlaboratory differences may not have played a significant role in the difference observed between Cheng's report and our results.

7. Conclusion

A CoMFA model has been developed with 48 compounds and validated by the use of 16 compounds not

present in the training set. This model correctly predicts the activities of most of the compounds in the test set. The test set molecules were then combined with those in the training set to obtain a final model which was evaluated to have a high predictive value ($R^2_{CV} = 0.732$) and a high regression coefficient ($R^2 = 0.989$; standard error = 0.135). This suggests that the basic hypothesis on which the model was built, i.e., the pharmacophore elements and the extended conformation of the phenylalkylamine moiety, has some validity. A few unique compounds were, however, incorrectly predicted. Amongst them was the most potent sigma ligand ever reported, SC 50691. The synthesis and the binding affinity constants obtained for SC 50691, and its *exo* and *endo* isomers were consistent with the model predictions and would suggest that the original report was in error. Analysis of the predictions also reveals a support for the hypothesis that phenylketones bind differently from phenylalkylamines and may have an additional binding interaction at the σ_1 receptor sites.

8. Experimental protocols

8.1. Synthesis

Proton magnetic resonance spectra were obtained with a GE QE-300 spectrometer with TMS as an internal standard. Spectral data are consistent with the assigned structures. Melting points were determined with a Thomas-Hoover melting point apparatus and are uncorrected. Elemental analysis was peformed by Atlantic Microlab and are within 0.4% of the theory.

8.1.1. 2-Piperidinobenzobicyclo[2.2.1]heptane, hydrobromide **65**

The methods of Schuster et al. [22] and Grunewald [20] were used. A solution of 1-bromo-2-iodobenzene (17 g, 6.0 mmol) and freshly generated cyclopentadiene [25] (8 g, 12.0 mmmol) in dried THF (90 mL) was added dropwise to magnesium turnings (1.5 g) in a three-necked flask under N_2. After the Mg turnings were fully immersed, the mixture was gently heated until reaction was initiated when the rest of the solution was added dropwise over a period of 1 h. The mixture was heated at reflux for an additional 0.5 h, then allowed to cool, solvent removed under reduced pressure, the residue was mixed with 30% NH_4Cl (50 mL) and extracted with ether (3 × 40 mL). The combined ethereal solution was dried ($MgSO_4$), solvent removed and the residue chromatographed over a column of Silica gel. The resulting oil was distilled (1 mm, 100 °C) to obtain a colorless oil; benzonorbornadiene (6.4 g, 75%). A solution of benzonorbornadiene (3 g, 2.1 mmol) in THF (5 mL) was added to a mixture of NaN_3 (4.1 g, 6.3 mmol) and $Hg(OAc)_2$ (6.6 g, 2.1 mmol) in 40 mL of 50% THF/H_2O solution. The resulting mixture was stirred at 50 °C for 18 h after which 3N NaOH (40 mL) and $NaBH_4$ {0.8 g in 3N NaOH (30 mL)} were added. Stirring was continued at room temperature for 1 h when the THF portion was separated and the aqueous portion was extracted with ether (3 × 40 mL). The combined organic solutions was evaporated under reduced pressure, redissolved in ether (20 mL) and dried ($MgSO_4$). The ethereal solution was subsequently added to a suspension of lithium aluminum hydride (2 g) in ether (50 mL) at 0 °C. The mixture was stirred at room temperature for 1 h and quenched by the cautious addition of drops of water. Work-up of the resulting mixture yielded an oily residue of the *exo* and *endo* isomers (as subsequently shown on TLC) which was purified by the formation of the hydrobromide salt and recrystalization from MeOH/ether (m.p.; 260-264 °C). The isomeric mixture (0.3 g, 1.2 mmol) in dried DMF (5 mL) was treated with 1,5-pentane dibromide in the presence of K_2CO_3 (0.42 g). After stirring for 24 h at 50 °C, a second portion of K_2CO_3 (0.21 g) was added and stirring continued for another 24 h. The reaction mixture was poured into cold water (50 mL) and then extracted with ether (3 × 30 mL). The combined organic portion was washed with H_2O (30 mL), dried ($MgSO_4$) and the HBr salt was prepared (90 mg, 23%). The salt was recrystallized from MeOH/ether: m.p. 272-275 °C (Dec.). Anal. ($C_{16}H_{22}NBr$): C,H,N.

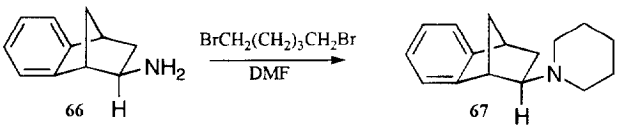

66 67

Figure 4. Synthesis of *exo*-2-piperidinobenzobicyclo[2.2.1] heptane.

8.1.2. Exo-2-Piperidinobenzobicyclo[2.2.1]heptane, oxalate **67** *(figure 4)*

Pentane-1,5-dibromide (0.5 g, 2.2 mmol) was added to a stirred mixture of *exo*-2-aminobenzonorbornene [20] (0.3 g, 1.9 mmol) and K_2CO_3 (0.3 g, 2.2 mmol) in dry DMF (15 mL). The reaction mixture was heated at 50 °C for 24 h. After cooling, the mixture was poured into cold water (25 mL); additional K_2CO_3 was added till pH > 10 and the mixture was extracted with ether (3 × 25 mL). The combined organic extracts were washed with water (25 mL), dried ($MgSO_4$), and evaporated. The resulting oil was purified by column chromatography on silica gel with $CHCl_3$, then $CHCl_3$–MeOH (9:1) as eluent, and the product was collected. The oxalate salt was prepared and recrystallized from a mixture of MeOH/Et_2O and finally from EtOAc to yield 150 mg (25%) of **67** as white crystals: m.p. 170-171 °C; ^{1}H-NMR (DMSO-d_6): δ 1.50-1.60 (br.s, 2H, CH_2); 1.70-1.85 (m, 6H, $3CH_2$), 2.15-2.30 (m, 2H, CH_2), 2.50 (d, 1H, C-3 *endo* H), 2.90-3.00 (m, 1H, C-2 *endo* H), 3.10-3.35 (m, 3H, CH_2+ C-3 *exo* H), 3.45 (s, 1H, bridgehead H), 3.90 (s, 1H, bridgehead H), 7.10-7.20 (m, 2H, ArH), 7.22-7.35 (m, 2H, ArH). Anal. ($C_{18}H_{23}NO_4$): C,H,N.

8.1.3. Endo-2-Piperidinobenzobicyclo[2.2.1]heptane, oxalate **69** *(figure 5)*

A mixture of piperidine (0.7 g, 8.2 mmol), benzonorbornenone [26] (0.25 g, 1.5 mmol), $NaCNBH_3$ (65 mg, 1 mmol) and 5 N methanolic solution of HCl (0.6 mL) in methanol (20 mL) was allowed to stir at room temperature for 72 h. The reaction mixture was concentrated under reduced pressure and the residue was taken up in water (15 mL) and washed with ether (15 mL). The aqueous solution was basified with KOH pellets to pH > 10, saturated with NaCl, and extracted with ether (3 × 15 mL). The combined organic extracts were dried ($MgSO_4$) and evaporated to dryness. The

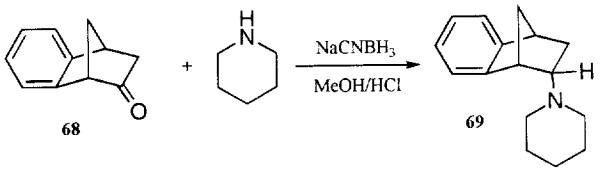

Figure 5. Synthesis of *endo*-2-piperidinobenzobicyclo[2.2.1] heptane.

residue was then purified by column chromatography using silica gel with $CHCl_3$-MeOH (9:1) as eluent to give the product as a clear pale yellow liquid. The oxalate salt was prepared and recrystallized from a MeOH/EtoAc mixture to give 100 mg (20%) of **69** as white crystals: m.p. 155-156 °C. ^{1}H-NMR ($CDCl_3$): δ 1.30-1.50 (br.s, 1H, C-3 *endo* H), 1.70-1.90 (m, 6H, $3CH_2$), 1.92-2.00 (m, 4H, $2CH_2$), 2.30-2.40 (m, 1H, C-3 *exo* H), 2.55-2.75 (br.s, 2H, CH_2), 3.40 (d, 1H, bridgehead H), 3.70 (S, 1H, bridgehead H), 3.75-3.80 (m, 1H, C-2 *exo* H), 7.15-7.35 (m, 4H, ArH). Anal. ($C_{18}H_{23}NO_4$): C,H,N.

8.2. Binding studies

The σ_1 radioligand-binding assay was carried out as previously reported [12] using (+)-[^{3}H]pentazocine as the radioligand. Approximately 100 mg of guinea pig membranes (prepared as previously described [3]), and (+)-[^{3}H]pentazocine (3-4 nM final concentration) in a final volume of 0.5 mL of 50 mM Tris-HCl buffer (pH 8.0). For the standard equilibrium essay, the mixtures were incubated for 4 h at 37 °C, the reactions quenched with 4 mL of ice-cold incubation buffer, and the mixtures rapidly filtered over Whatman GF/B or Schleicher & Scheull no. 32 glass fiber filters followed by three 4-mL rinses with additional ice-cold buffer. The radioactivity on the filters was determined by scintillation spectrometry at an efficiency of about 50%. Nonspecific binding was determined in the presence of 10 mM haloperidol. IC_{50} values were determined from competitive curves using nonlinear least-squares regression analysis and converted to K_i values with the Cheng-Prusoff transformation. Each K_i value was determined from three to five separate determinations.

Acknowledgements

We acknowledge the financial support by the Cambridge NeuroScience, Inc. This work is also supported in part by a grant from the National Institute of Health, Division of Research Resources, MBRS program, Grant # GM 08111 and the RCMI Grant # G12 RR 03020.

References

[1] Walker J.M., Bowen W.D., Walker F.O., Matsumoto R.R., de Costa B., Rice K.C., Pharmacol. Rev. 42 (1990) 355-403.

[2] Abou-Gharbia M., Ablordeppey S.Y., Glennon R.A., Ann. Rep. Med. Chem. 28 (1993) 1-10.

[3] Moebius F.F., Striessnig J., Glossmann H., Trends Pharmacol. Sci. 18 (1997) 67-70, and references therein.

[4] Glennon R.A., Smith J.D., Ismaiel A.M., El-Ashmawy M.B., Battaglia G., Fischer J.B., J. Med. Chem. 34 (1991) 1094-1098.

[5] Glennon R.A., Yousif M.Y., Ismaiel A.M., El-Ashmawy M.B., Herndon J.L., Fischer J.B., Server A.C., Burke Howie K.B., J. Med. Chem. 34 (1991) 3360-3365.

[6] El-Ashmawy M.B., Ablordeppey S.Y., Hassan I., Gad L., Fischer J.B., Burke Howie K.B., Glennon R.A., Med. Chem. Res. 2 (1992) 119-126.

[7] Ablordeppey S.Y., Fischer J.B., Burke Howie K.B., Glennon R.A., Med. Chem. Res. 2 (1992) 368- 375.

[8] Ablordeppey S.Y., Issa H., Fischer J.B., Burke Howie K.B., Glennon R.A., Med. Chem. Res. 3 (1993) 131-138.

[9] Ablordeppey S.Y., El-Ashmawy M.B., Glennon R.A., Med. Chem. Res. 1 (1991) 425-438.

[10] Glennon R.A., Ablordeppey S.Y., Ismaiel A.M., El-Ashmawy M.B., Fischer J.B., Burke Howie K.B., J. Med. Chem. 37 (1994) 1214-1219.

[11] Rothman R.B., Reid A., Mahboubi A., Kim C., de Costa R.R., Jacobson A.E., Rice K.C., Mol. Pharmacol. 39 (1991) 222-232.

[12] Fischer J.B., Burke Howie K.B., Dunn J.A., Ablordeppey S.Y., Glennon R.A., Soc. Neurosci. Abstr. 18 (1992) 455.

[13] Berardi F., Colabufo N.A., Giudice G., Perrone R., Tortorella V., Govoni S., Lucchi L., J. Med. Chem. 39 (1996) 176-182.

[14] Berardi F., Giudice G., Perrone R., Tortorella V., Govoni S., Lucchi L., J. Med. Chem. 39 (1996) 4255-4260.

[15] Newman A.H., Shah J.H., Izenwasser S., Heller B., Mattson M., Tortella F.C., Med. Chem. Res. 6 (1996) 102-117.

[16] Xiao-shu H., Bowen W.D., Lee K.S., Williams W., Weinberger D.R., de Costa B.R., J. Med. Chem. 36 (1993) 566-571.

[17] Zhang Y., Williams W., Bowen W.D., Rice K.C., J. Med. Chem. 39 (1996) 3564-3568.

[18] Cramer III RD., Patterson D.E., Bunce J.D., J. Am. Chem. Soc. 110 (1988) 5959-5967.

[19] Cheng B.K., Gray N.M., Contreras P.C., Bremer M.E., Christine L.J., Abstr. # 17, 200th Am. Chem. Soc. Meeting, Div. Med. Chem., Washington D.C., August 26-31, 1990.

[20] Grunewald G.L., Reitz T.J., Hallett A., Rutledge C.O., Vollmer S., Archuleta III J.M., Ruth J.A., J. Med. Chem. 23 (1980) 614-620.

[21] Borch R.F., Bernstein M.D., Durst H.D., J. Am. Chem. Soc. 93 (1971) 2897-2904.

[22] Schuster D.I., Katerinopoulos H.E., Holden W.L., Narula A.P.S., Libes R.B., Murphy R.B., J. Med. Chem. 25 (1982) 850-854.

[23] de Costa B.R., George C., Burke Jr. T.R., Rafferty M.F., Contreras P.C., Mick S.J., Jacobson A.E., Rice K.C., J. Med. Chem. 31 (1988) 1571-1575.

[24] Gulligan P.J., Cain G.A., Christos T.E., Cook L., Drummond S., Johnson A.L., Kergaye A.A., McElroy J.F., Rohrbach K.W., Schmidt W.K., Tam S.W., J. Med. Chem. 35 (1992) 4344-4361.

[25] Moffet R.B., In: Organic Synthesis Collection, Vol. IV, Wiley, New York, 1963, p. 238.

[26] Kleinfelter D.C., von Shleyer P.R., In: Organic Synthesis Collection, Vol. V, Wiley, New York, 1973, p. 852.